RSC Advances

PAPER

View Article Online
View Journal | View Issue

Cite this: *RSC Adv.*, 2020, **10**, 21

Flexible pH sensor based on a conductive PANI membrane for pH monitoring

Yongqian Li, *[ab] Yunlong Mao,[b] Chi Xiao,[b] Xiaoli Xu[c] and Xueyong Li*[c]

Received 6th November 2019
Accepted 11th December 2019

DOI: 10.1039/c9ra09188b

rsc.li/rsc-advances

pH is a critical parameter used to specify the acidity or alkalinity of an aqueous solution in chemistry, food processing, and medical care. In this study, a conductimetric-type micro pH sensor has been achieved using PANI membrane fabricated on a flexible substrate film aiming to monitor wound healing. The sensor is based on the incorporation of a polyaniline (PANI) membrane, interdigital electrode, and polyimide (PI) substrate. PANI was doped with dodecyl benzene sulfonic acid (DBSA) to obtain good conductivity. The electrodes were patterned on the PI film by etching. The contact area between the PANI and interdigital electrodes improves the responsiveness of the pH sensor. A sensitivity of 58.57 mV per pH over the entire pH range from 5.45 to 8.62 was obtained experimentally, along with a superior repeatability of 8% FS (full scale) and a temperature drift of 6.8% FS. This micro flexible pH sensor aims to monitor the pH value of wound healing, which also facilitates the realization of online monitoring of the pH for telemedicine, food safety, and home health care.

1. Introduction

pH, which is defined as a logarithmic measure of the hydrogen ion concentration,[1] is an essential analytical measure of the mechanism of chemical or biological reactions in a broad range of applications, including environmental, industrial, and biomedical conditions. pH sensors play a critical role in most continuous chemical processes to ensure the reaction quality[1,2] and to monitor health.[3,4]

pH sensors are classified based on their working principle as potentiometric, capacitive, or optical. Typically, potentiometric pH sensors consist of a working electrode and a reference electrode. For example, Rahimi *et al.* developed a potentiometric type of pH sensor that utilizes an Ag/AgCl reference electrode and a carbon electrode coated with a polymeric membrane as the sensitive electrodes.[5] Mature commercial potentiometric pH sensors are usually based on a rigid electrode or on a Si substrate.[6,7] The disadvantages of both the bulky electrode and single-point diagnostic limit their application in the wearable medical field. To improve the detection sensitivity and reduce the working volume, ion sensitive field effect transistors (ISFETs) have been proposed as a new type of pH sensor. These sensors adjust the threshold voltage by an ion-sensitive field effect and consequently change its current–voltage output.[8] Recently, paper-based analytical devices (PADs) have been able to indicate pH by employing color changes,[9] which have shown excellent superiority because of their easy fabrication and point-of-care assay platforms.[10] Optical sensors can indicate the presence of specific ions by changing their optical properties, such as the fluorescence intensity.[1] These optical pH sensors are often used to monitor the water content or organic solvents.[1,2,11] A two-photon fluorescent sensor can image living cells by detecting the pH fluctuation in tumor diagnosis.[12] However, optical pH sensors need an external image camera or light detector to function, which is considerably inconvenient for clinic applications.

Recently, flexible sensors have received considerable attention for the continuous monitoring of human health.[13,14] To meet the special demands in fields, such as wearable electronics, electronic skin, and neuronal implants, various sensors on flexible substrates have been realized.[15] In particular, the updated MEMS (Micro-Electro-Mechanical System) fabrication technologies have enabled the realization of various flexible sensors.[16,17] One important application of wearable electronics is clinical treatment for wound dressing.[18] The period of wound healing can range from a few months to even years. To avoid frequently changing a surgical dressing, wound dressings employing a pH sensor and other smart sensors can be used to monitor the wound state.[19] Additionally, to endure the requirements of repetitive mechanical deformation as is the case with wearable and epidermal sensors, flexibility must be taken into account to ensure non-invasive comfortability, which is a critical requirement for real-time pH monitoring.[19,20] For this purpose, the conformal nature of commercially available temporary transfer papers[21,22] and textile sensors[23] have been used for real-time monitoring of epidermal pH levels. Most of

[a]*Research & Development Institute of Northwestern Polytechnical University in Shenzhen, Shenzhen 518000, China. E-mail: liyq@nwpu.edu.cn*

[b]*Key Laboratory of Micro/Nano Systems for Aerospace of Ministry of Education, Northwestern Polytechnical University, Xi'an, Shaanxi 710072, China*

[c]*Department of Burn and Plastic Surgery, Tangdu Hospital, Air Force University, Xi'an 710038, China. E-mail: yuyong@fmmu.edu.cn*

these sensors can satisfy the operational metrics (*i.e.*, sensitivity, resolution, and dynamic range). For promoting wound healing and scar inhibition, a pH sensor must work in a humid treatment environment.[5,18,19]

In this study, we developed a flexible pH sensor to monitor real-time pH levels for wound healing assessment in which a large effective area improves the sensitivity up to 58.57 mV per pH, and the polymer substrate film enables a flexibility of less than 5%. Different from the potential type based on the electron transfer in redox reaction, the sensor developed in the article works based on the electron migration passing through a pH responsive polyaniline (PANI) membrane, which obey Ohm's law. The pH fluctuations of any point on the surface of the PANI sensing membrane leads to a corresponding increase or decrease in the mobility of the ions, resulting in changes in the sensor resistance. During the measurement, the sensor was powered with a constant current through the interdigital electrodes. The resistance of membrane varies when contacting analytes with different pH, leading to the output voltage changes.

Furthermore, the common potential-type sensors consist of two different electrodes, working electrode which contains the sensitive material and reference electrode which is always Ag/AgCl electrode.[5,24] Only the working electrode is effective sensitive area. The effective sensitive area of our developed sensor is the full area of PANI membrane, which means our sensor takes larger proportion of effective sensitive area.

Our sensors were fabricated by MEMS techniques, including etching electrodes on a flexible polyimide film and spin coating the PANI membrane on planar interdigital electrodes. The flexible polyimide (PI) membrane enables our sensors to work under clinical wound healing conditions to eliminate patient discomfort. Compared with optical pH sensors, this conductimetric-based sensor is more suitable for real-time monitoring without auxiliary electrodes. The sensitive area of the PANI sensing surface was optimized to be small enough to ensure both comfortable wearability and increasing sensitivity. In addition, the PANI membrane can work in wet environments. The performance and characteristics satisfy the requirements for practical scenarios of epidermal monitoring during wound healing.

2. Materials and methods

Fig. 1 shows a schematic of our pH sensor. One sensor consists of a PANI membrane layer as the sensitive element, the interdigital electrode as the transmission layer, and PI membrane as the substrate film. Each layer of the sensor is less than 30 μm thick; thus, the entire sensor is still a membrane with a thickness of less than 100 μm. In Fig. 1, the reversible protonation process in acid and the deprotonation process in basic of doped PANI were demonstrated. We elaborated the meaning of symbols with the legend on the right side. Two arrows and little light blue circular describe the H^+ transfer process on the PANI membrane. In acid solutions, the polymer is doped with H^+ ions to create the emeraldine salt (ES) form of PANI, which is highly electrically conductive. The resulting surface charge decreases the resistance, leading to a voltage change. When the polymer is exposed to basic solutions, the captured H^+ ions are neutralized by OH^-, resulting in the opposite effect. The Fig. 2 presented the protonation–deprotonation pathway of PANI.

2.1 Reagents

The analytical aniline monomer, dodecyl benzene sulfonic acid (DBSA), reagent grade ammonium persulfate ($(NH_4)_2S_2O_8$), acetone, and PVA (polyvinyl alcohol) were purchased from Aladdin. PI a thickness of 12.5 μm was purchased from Meixin Insulation Materials Co., Ltd.

2.2 Design and fabrication of the interdigital electrode

Interdigital electrodes have been widely used to improve the sensitivity of different kinds of sensors.[16,25–28] Interdigital electrodes are applied in the biological and chemical sensors, when the biochemical molecule or chemical analytes were directly attached to the surface of interdigital electrodes.[25] Often interdigital electrodes are utilized to obtain the conductimetric quantity variation of the sensitive medium when no direct chemical reaction produced. The voltage varying results from the changes in the resistance of sensing materials, such as in hydrogel,[26] or tin oxides (SnO and SnO_2).[27] The discrepancy between potentiometric and conductimetric type was the electrode configure. At least two different materials are used in potentiometric electrodes, two identical electrodes in conductimetric one.[27] The output voltage changing in interdigital electrode type sensors can also result from the capacitance varying in a electrochemical sensors.[28] In this article, the resistance change of the PANI membrane was transformed into the voltage variation when a constant current passing through.

Obviously, the resistive interface between the PANI membrane and interdigital electrodes determine the properties of the sensor. A smaller initial resistance will give rise to a higher relative sensitivity.[29,30] In order to minimize the initial resistance of the whole sensor, we simulated the resistance of interdigital electrodes. The simulation calculations were performed by using commercial software. As shown in Fig. 3, for PANI-based pH sensors, the width and length of a single interdigital electrode are negatively correlated with the resistance. However, the longitudinal and transverse sizes of the interdigital electrodes positively determine the initial resistance. Decreasing the thickness of each interdigital electrode increases the initial resistance. These results are not exactly consistent with the dependence of the sheet resistance on its dimensional size; however, they have a similar trend.

The electric properties were also calculated by focusing the signal-to-noise ratio of the output voltage and amplitude.

We found that reducing the longitudinal distance between the interdigital electrodes can improve the signal-to-noise ratio of the output voltage signal and increase the signal amplitude. For wearable epidermal sensors, the smaller the sizes and the volume, the better the comfort and the dynamic response. However, for the actual parameters of the interdigital electrode, the process technologies must be considered for easy fabrication.[31]

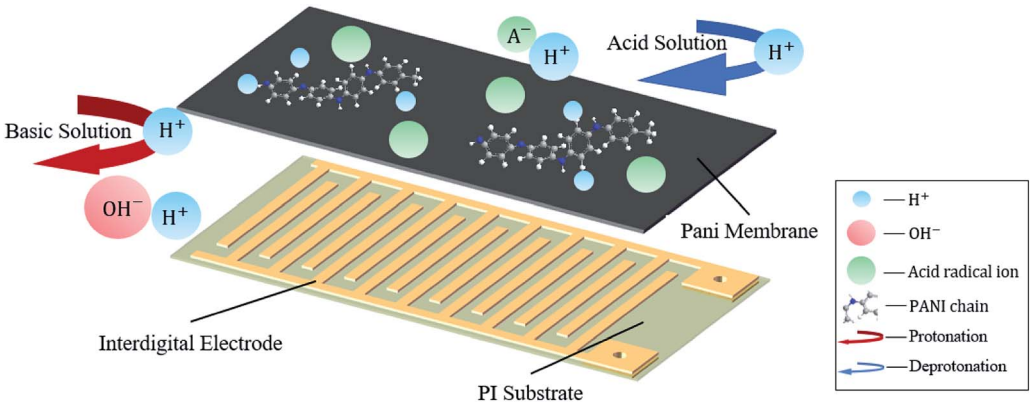

Fig. 1 A schematic representation of our pH sensor consisting of a PANI membrane on interdigital electrodes supported by a PI substrate. The transformation of PANI protonated in acid solution and deprotonated in basic solution.

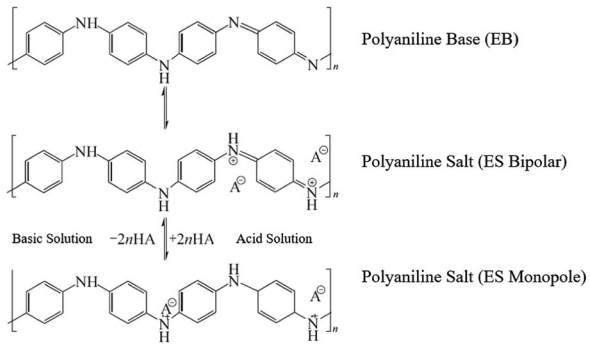

Fig. 2 Scheme of polyaniline protonation–deprotonation pathway.

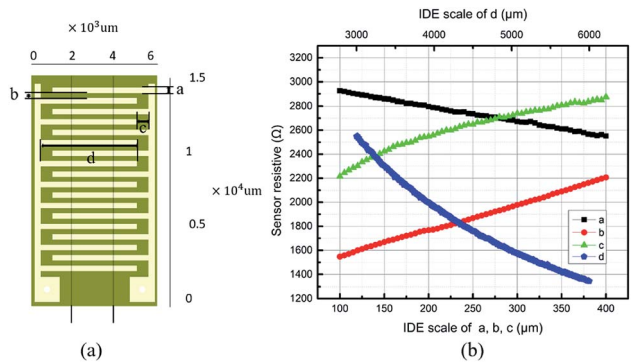

Fig. 3 Improved design of an interdigital electrode (IDE) for a pH sensor. (a) Schematic representation of a generic interdigital electrode showing the geometric parameters. (a – width, b – longitudinal spacing; c – transverse spacing; d – finger length). (b) The initial resistance of the IDE depends on the geometric parameters. The increasing sizes of the longitudinal (red line) and transverse (green line) spacing enhance the initial resistance, whereas both the grid width (black line) and the length (blue line) weaken the initial resistance.

The patterns of the interdigital electrodes were fabricated following the process shown in Fig. 4(a). A copper layer with a thickness of 25 μm was pressed tightly with a hot press on both sides of a PI film. Holes were drilled and the activation of the hole wall was plated to settle the copper membrane on the entire wall. Pickling and micro-etching enabled the formation of a microroughness in the surface of the copper film to increase the adhesion strength.[31] The layout of the interdigital electrode array was printed into a photopolymerization dry film for lithography etching. Sodium carbonate was used to remove the residuary dry film. The resulting metallic structures of the

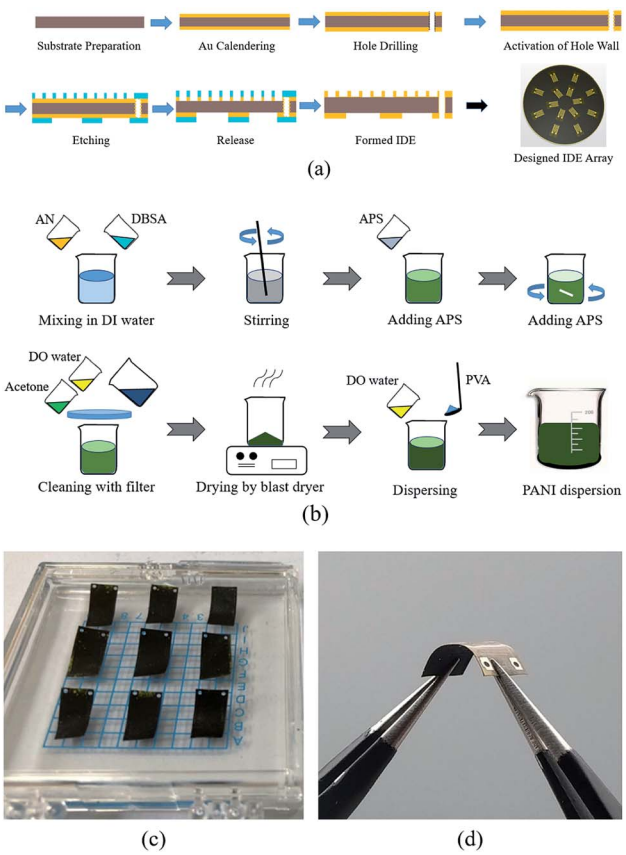

Fig. 4 The fabrication processes of the pH sensor. (a) Process for the PANI membrane preparation. (b) Fabrication process for the interdigital electrodes. (c) Photograph of a group of our fabricated sensors. (d) A sensor bent at approximately 135°.

interdigital electrodes were obtained on the PI substrate, as shown in Fig. 4(a).

2.3 Fabrication of the conductive PANI

Many conductive polymers have been investigated for chemical sensing.[4,7] Among those conductive polymer materials, PANI has attracted a considerable amount of attention because of its conjugated electronic structure and its good electrical conductivity. Additionally, PANI can be easily doped or dedoped using an acid.[32,33] PANI is an attractive pH-sensitive candidate because it is an intrinsically pH-sensitive polymer with good environmental stability. A PANI detector integrated in a microfluidic device has been reported for dynamic pH imaging and mapping.[34] The provision of an inherent response to the pH change in a continuous flush flow offers the possibility of real-time pH monitoring.

The conductivity of PANI associated with the reversible emeraldine salt (ES)–emeraldine base (EB) transition has led to its widespread application in solid-state pH sensors.[17] The intrinsic conductivity of PANI is considerable affected by the doping process. Furthermore, the minimal cytotoxicity of PANI results in negligible skin irritation.[22]

The reagents and method for PANI fabrication, as shown in Fig. 4(b), involved aniline monomer, dodecyl benzene sulfonic acid (DBSA), and ammonium persulfate (APS). First, the aniline monomer and dodecyl benzene sulfonic acid were mixed in deionized water with magnetic stirring in a water bath at a constant temperature.

To further improve the dissolvability, the mixture was ultrasonic dispersed for approximately 3 min. Then, ammonium persulfate (approximately 0.1 mol) was slowly added to the mixture. Then, deionized water was added to the mixture until the total volume reached 200 mL, which ensured that all reagents completely dissolved. After stirring in a constant temperature water bath for 24 h, the mixture solution became a dark green suspension. To obtain the pure powder, a G4 sand core funnel, acetone, and deionized water were used to filter and clean the suspended substance until the PANI dispersive solution became colourless. Finally, the compound was dried to obtain the pure conductive PANI powder.

2.4 Spin coating process for the PANI membrane

Spin coating is the key process for integrating the sensitive PANI membrane with the IDE array on a PI substrate film. Mass fabrication can be realized using the spin coating method. The preparation of the PANI dispersion solution is as follows. The PANI powder and PVA were ultrasonically dispersed in deionized water. After experiments and comparison, the weight ratio of the PANI powder, polyvinyl alcohol, and the entire dispersion was set as 1 : 5 : 10. The dispersion solution was fully stirred using a magnetic stirrer at 40 °C for 4 h, and air bubbles in the dispersion solution were extracted using a vacuum furnace.

The great flexibility of the electrode arrays on the polyimide substrate makes spin coating impossible. We used a silicon wafer as a solid substrate for the spin coating process. To retain the hydrophilicity of the silicon wafer, the RCA process was used to remove the organic residue, metal ionic contaminants, and the native oxide layer from the silicon wafer, leaving a pure silicon surface.[31] The polyimide substrate with the flexible electrode array was softly stuck on the moistened surface of the silicon wafer. The spin coating process produces a PANI membrane on the surface of the IDE array. The silicon wafer was stuck on the rotary table using a vacuum chuck. The PANI dispersion solution was syringed onto the surface of the IDE array.

The spin coating process was performed following three successive steps: a rotational speed of 50 rpm for 30 s, 100 rpm for 60 s, and 500 rpm for 120 s. In the interval between spin coating steps, the sample was vacuumed in a vacuum drying oven for 120 s to remove air bubbles within the PANI membrane. The fabricated sensors are shown in Fig. 4(c), and the flexibility is shown in Fig. 4(d).

After spin coating, the PANI was dispersed on the surface of interdigital electrodes and in their gaps. The membrane was then dried and cured in thermostat for 12 hours at room temperature. Finally, the membrane was cut into separate chips as shown in Fig. 4(c).

A constant current was applied through the circuit. The voltage changes of the sensor were obtained once the resistance of the PANI membrane changed due to the analytes contacting.

2.5 Voltage measurements

Our fabricated pH sensors were evaluated by employing buffer solutions at different pH levels of 5.45, 6.86, 7.70, and 8.62. Potassium dihydrogen phosphate (KH_2PO_4) and anhydrous sodium hydrogen phosphate (Na_2HPO_4) were dissolved in deionized water firstly. Then, the mixed solution was diluted into different solutions with the required concentration by adding drops of 0.1 mol per L HCl or 0.1 mol per L NaOH. A standard pH meter (LiChen-pH-100, range from pH 0.00 to 14.00 with an uncertainty of $\pm$0.01) was used to calibrate the homemade buffer solution in the laboratory. The calibrated range from 5.45 to 8.62 was in the relevant pH range of pH 5.5 to 9 for clinical wound healing.[24,35]

Before the experiments, two wires were attached to the reserved pads on the back side of PI substrate. The current passing through the PANI membrane was powered by an Agilent power source (Agilent B2962A).

The measurements of output voltage changes were collected using data acquisition software *via* a Tektronix oscilloscope (Tektronix MDO 3024). For each test, the data was recorded after the sensor immersed in pH buffer for 90 seconds. The sensors were immersed sequentially in adequate buffers with different pH levels without concerning cross-contamination.

2.6 Morphology measurements

During fabrication process, the quality of the PANI–PVA compound was measured by optical microscope (PRECISE Axio Lab. A1). The morphology of the final membrane was evaluated by scan electron microscope (TESCAN VEGA 3LMU).

Before the spin coating, the PANI–PVA compound was dispersed uniformly in deionized water after 4 hours of stirring.

The mixing state of the PANI–PVA samples was then observed by optical microscope under 100×, as shown in Fig. 5(a). The PANI–PVA clusters were dispersed with uniformity in the deionized water.

After curing, the morphology of the membrane was observed by scan electron microscope with an acceleration voltage of 3 kV. The surface of cured PANI membrane was uniform as shown in Fig. 5(b).

3. Results and discussion

3.1 Sensitivity

Sensitivity is defined as the slope of the transfer function of a sensor. As shown in Fig. 6(a), the sensitivity was calibrated from the fitting lines obtained for the different fabricated sensors. The transfer function can be obtained by the linearization, which is approximates the actual curve with a straight line within the range obtained by the overall error. Among the methods, the least square fitting method is more accurate, and the calculation method is as follows.[36]

$$m = \frac{n\sum_{i=1}^{n} x_i y_i - \sum_{i=1}^{n} x_i \sum_{i=1}^{n} y_i}{n\sum_{i=1}^{n} x_i^2 - \left(\sum_{i=1}^{n} x_i\right)^2} \quad (1)$$

$$b = \frac{\sum_{i=1}^{n} x_i^2 \sum_{i=1}^{n} y_i - \sum_{i=1}^{n} x_i \sum_{i=1}^{n} x_i y_i}{n\sum_{i=1}^{n} x_i^2 - \left(\sum_{i=1}^{n} x_i\right)^2} \quad (2)$$

In fitting formulas (1) and (2), m is the slope of the fit line, b refers to the intercept of the fit line. The slopes of the three calibrated lines were 60.14 mV per pH, 58.84 mV per pH, and 56.73 mV per pH. The corresponding intercepts were 347.04, 356.11, and 368.69, respectively. The results obtained in Fig. 4(a) yielded an average sensitivity of 58.57 mV per pH (2.398% RSD), which is regarded as the sensitivity of our developed pH sensor. Herein, RSD refers to the relative standard deviation, which is also a significant characteristic.[24] This sensitivity of 58.57 mV per pH meets the requirements for epidermal pH monitoring in wound healing, as indicated by previous studies.[7,22] In our conductimetric-type pH sensor, sensitivity is not restricted by the Nernstian slopes that are used for potentiometric-type sensors.[7,21,24]

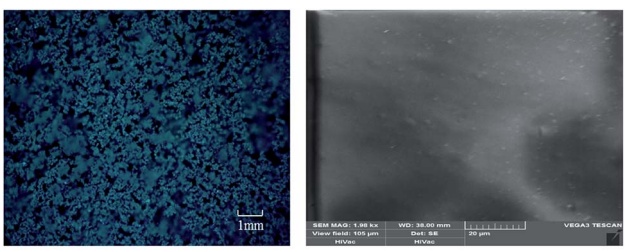

(a) (b)

Fig. 5 The morphology of fabrication sensor. (a) The uniform mixing state of the PANI, PVA and deionized water, and (b) the fabricated membrane surface.

3.2 Hysteresis

The hysteresis, which indicates the degree of inconsistency between the increasing and reverse loading, was also tested in our experiments. The calculation formula of the hysteresis is as follows:[37]

$$\delta_h = \frac{\Delta H_{max}}{y_{FS}} \times 100\% \quad (3)$$

where ΔH_{max} is the maximum error between increasing loading and the decreasing loading and y_{FS} is the theoretical full scale. The sensors were evaluated by immersing them in solutions of different pH levels sequentially with no cleaning or other treatment in the interim. The output response during the forward and reverse changes in the pH buffer solutions is depicted in Fig. 6(b). The pH sensor displayed a nearly instantaneous response to pH changes, confirming the fast and reversible transition between the emeraldine salt (ES) and the emeraldine base (EB). According to the formulas (3), the hysteresis was less than 12% FS. Here, FS refers to the full scale.[37] The hysteresis is mainly due to the cross-contamination between measurements[24] and inadequate deprotonation during experiment. The hysteresis is also defined by the EMF variation in addition to the variation in pH.[17]

3.3 Repeatability

Repeatability indicates the degree of inconsistency of the output of the sensor under the same working conditions several times through the entire range.

The calculation formula of repeatability is as follows:[38]

$$\delta_r = \frac{\mathrm{Max}(\Delta_r)}{y_{FS}} \times 100\% \quad (4)$$

where Δ_r is the maximum error among the obtained data and y_{FS} is the full scale in theory.

The results for obtaining repeatability in our experiment are displayed in Fig. 6(c). According to formula (4), the repeatability of the sensor was determined to be 8% FS.

3.4 Temperature drift

For medical applications, it is important to evaluate the sensors at varying temperatures that are physiologically relevant.[14] The temperature drift is defined as follows:

$$\delta_s = \frac{\mathrm{Max}(\Delta_s)}{y_{FS}} \times 100\% \quad (5)$$

where Δ_s is the error obtained during the temperature fluctuation. Fig. 7(a) shows the response of the pH sensor upon change in temperature from 30 °C to 40 °C, which indicates an average temperature drift of 6.8% FS.

The temperature drift of a potentiometric-type sensor is predicted by the Nernstian equation, which is caused by the changes in (RT/F) pH.[15,17] Such temperature drifts are also acceptable for wound healing applications.[5]

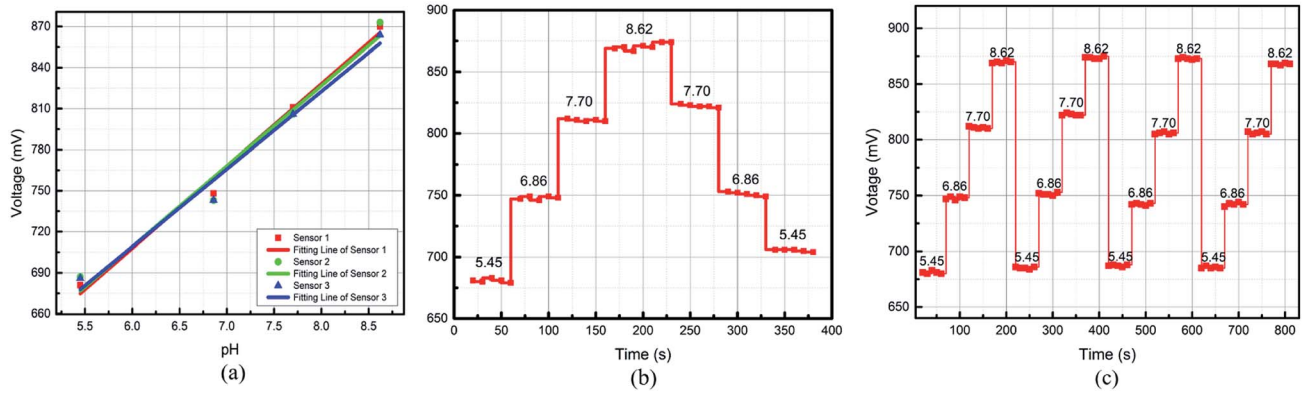

Fig. 6 Sensor response for a group of discrete pH levels from pH 5.45 to pH 8.62. (a) The fitting lines of the three sensors show the linear response with an average sensitivity of 58.57 mV per pH (2.398% RSD). (b) The output response of a pH sensor for increasing and reverse pH buffer solutions. (c) Repetitive results for a group with increasing pH.

3.5 Flexibility

For valid wound healing monitoring, a pH sensor needs to work under bending conditions.

The output voltage as a function of different bending angles from 0° to 90° was measured. As shown in Fig. 7(b), the voltage change increased slightly with the increasing bending angle and bending cycles. However, the voltage variation was within 5% FS after a sensor was bent 20 times even the case of approximate 90° bending angle. The flexibility of the pH sensor exhibited good stability, which makes it suitable for epidermal wound healing monitoring in clinical applications.

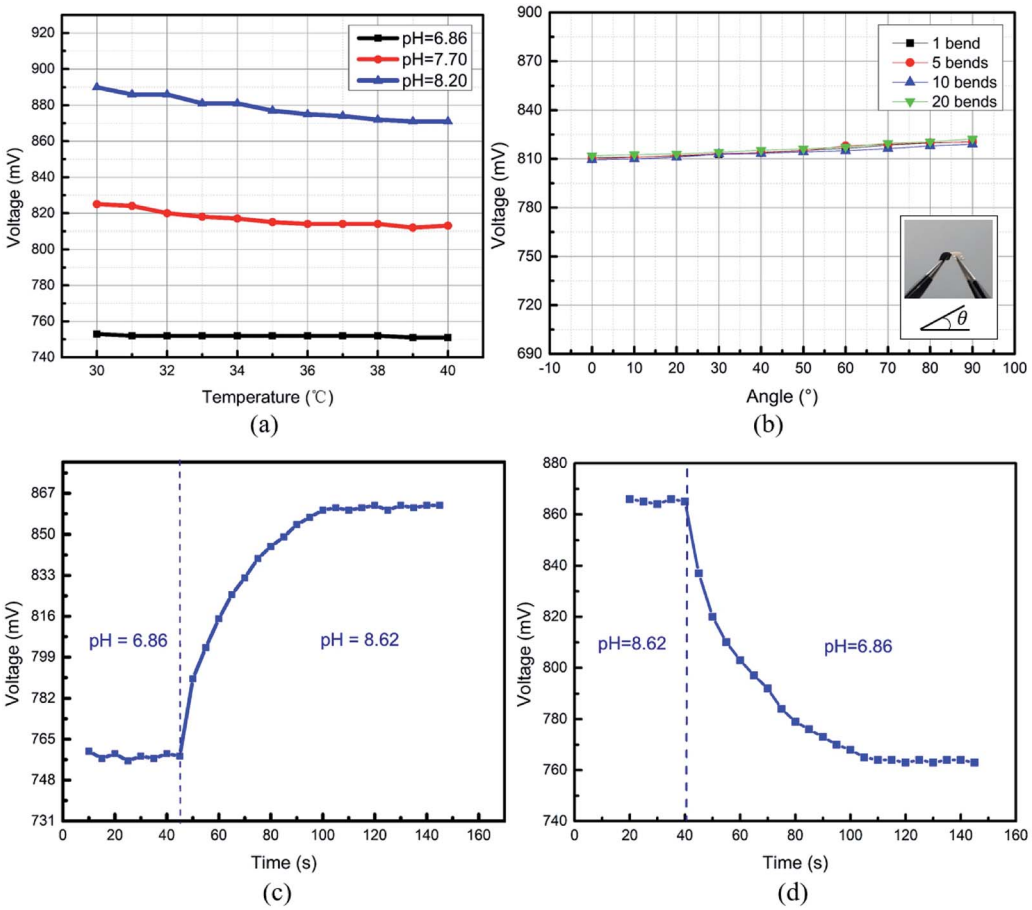

Fig. 7 (a) Flexibility experiments of the pH sensors. (b) Temperature effect of the pH sensors upon varying the temperature from 30 °C to 40 °C for three different pH levels. The dynamic response of the pH sensor for a step pH change shows (c) a rising time from pH 6.86 to 8.62 and (d) an inverse fall time from pH 8.62 to 6.86.

3.6 Response time

Fig. 5 shows the response time of the pH sensors for step pH changes from 6.0 to 8.0 and a reverse step change. Fig. 7(c) shows the response time of 45 s for an increasing process from pH 6.0 to 8.0, and a fall time of 54 s was observed, as shown in Fig. 7(d). The reduction in the thickness of the PANI membrane deposited on the surface of IDE would lead to a shorter response time.[38] Previous work on a PANI-based pH-sensitive electrode-type sensor has shown a faster response time (a few seconds), which was due to a thinner PANI layer being deposited *via* electro-deposition.[39] The spin coating technique, in contrast, produces thicker films, resulting in a longer response time. The obtained response time for our pH sensors is adequate for medical care applications and other clinical settings.[5,18]

4. Conclusions

Although further work is still required to fully validate the sensors under practical scenarios and to address the intercept variability, these attractive performances make this sensor well suited for developing biocompatible sensors that are relevant to wearable epidermal non-invasive monitoring.

For real-time monitoring of pH levels in wound healing applications, a conductimetric-type of micro pH sensor was developed using PANI membrane fabricated on a flexible substrate, which is different with the potential-type pH sensor, where both working and reference electrodes are required. Both the doped PANI membrane with sensing elements and the optimized structures of the interdigital electrodes improved the sensitivity to 58.57 mV per pH. The attractive figures of merit of the fabricated sensors were a temperature drift of 6.8% FS and a bending variation within 5% FS. The dynamic responses include a resulting rise time of less than 45 s and a fall time of 54 s. The mechanical characteristics of the resulting PANI membrane withstood repeated bending.

Additionally, owing to the merit of direct voltage output, this flexible and micro pH sensor has the potential to work as part of the wireless devices.[40]

Conflicts of interest

There are no conflicts to declare.

Acknowledgements

This work is funded by Foundation for Basic Research from Science and Innovation Commission of Shenzhen Municipality, China (JCYJ20170306153605871), the National Natural Science Foundation of China (No. 51575455), and the Tangdu Hospital Science and Technology Innovation Development Fund (2015JSYJ001, 2018JSYJ001).

Notes and references

1 D. Wencel, T. Abel and C. McDonagh, *Anal. Chem.*, 2014, **86**, 15–29.
2 Y. Qin, H.-J. Kwon, M. M. R. Howlader and M. J. Deen, *RSC Adv.*, 2015, **5**, 69086–69109.
3 J. Kim, A. S. Campbell, B. E. de Avila and J. Wang, *Nat. Biotechnol.*, 2019, **37**, 389–406.
4 T. R. Dargaville, B. L. Farrugia, J. A. Broadbent, S. Pace, Z. Upton and N. H. Voelcker, *Biosens. Bioelectron.*, 2013, **41**, 30–42.
5 R. Rahimi, M. Ochoa, T. Parupudi, X. Zhao, I. K. Yazdi, M. R. Dokmeci, A. Tamayol, A. Khademhosseini and B. Ziaie, *Sens. Actuators, B*, 2016, **229**, 609–617.
6 I. Tubía, F. Carazo, A. Apezteguía, E. Pérez-Lorenzo, J. Paredes and S. Arana, *Sens. Actuators, A*, 2018, **277**, 1–7.
7 R. D. A. A. Rajapaksha, U. Hashim, S. C. B. Gopinath and C. A. N. Fernando, *Microsyst. Technol.*, 2017, **24**, 1965–1974.
8 C. Jimenez-Jorquera, J. Orozco and A. Baldi, *Sensors*, 2010, **10**, 61–83.
9 C. Pinyorospathum, P. Rattanarat, S. Chaiyo, W. Siangproh and O. Chailapakul, *Sens. Actuators, B*, 2019, **290**, 226–232.
10 A. W. Martinez, S. T. Phillips, G. M. Whitesides and E. Carrilho, *Anal. Chem.*, 2010, **82**, 3–10.
11 *pH of Water*, https://www.fondriest.com/environmental-measurements/parameters/water-quality/ph/, accessed 10.12.2019.
12 F. Wang, D. Liu, Y. Shen, J. Liu, D. Li, X. Tian, Q. Zhang, J. Wu, S. Li and Y. Tian, *Dyes Pigm.*, 2019, **166**, 92–97.
13 A. J. Bandodkar, I. Jeerapan and J. Wang, *ACS Sens.*, 2016, **1**, 464–482.
14 W. Gao, S. Emaminejad, H. Y. Y. Nyein, S. Challa, K. Chen, A. Peck, H. M. Fahad, H. Ota, H. Shiraki, D. Kiriya, D. H. Lien, G. A. Brooks, R. W. Davis and A. Javey, *Nature*, 2016, **529**, 509–514.
15 J. Heikenfeld, A. Jajack, J. Rogers, P. Gutruf, L. Tian, T. Pan, R. Li, M. Khine, J. Kim, J. Wang and J. Kim, *Lab Chip*, 2018, **18**, 217–248.
16 N. F. Sheppard Jr, M. J. Lesho, P. McNally and A. Shaun Francomacaro, *Sens. Actuators, B*, 1995, **28**, 95–102.
17 X. Zhang, B. Ogorevc and J. Wang, *Anal. Chim. Acta*, 2002, **452**, 1–10.
18 R. S. Ambekar and B. Kandasubramanian, *Eur. Polym. J.*, 2019, **117**, 304–336.
19 G. C. Gurtner, S. Werner, Y. Barrandon and M. T. Longaker, *Nature*, 2008, **453**, 314–321.
20 S. Nakata, M. Shiomi, Y. Fujita, T. Arie, S. Akita and K. Takei, *Nat. Electron.*, 2018, **1**, 596–603.
21 L. Fonseca, M. Prunnila, E. Peiner, A. Moya, M. Zea, E. Sowade, R. Villa, E. Ramon, R. R. Baumann and G. Gabriel, *presented in part at the Smart Sensors, Actuators, and MEMS VIII*, 2017.
22 A. J. Bandodkar, V. W. Hung, W. Jia, G. Valdes-Ramirez, J. R. Windmiller, A. G. Martinez, J. Ramirez, G. Chan, K. Kerman and J. Wang, *Analyst*, 2013, **138**, 123–128.
23 D. Morris, S. Coyle, Y. Wu, K. T. Lau, G. Wallace and D. Diamond, *Sens. Actuators, B*, 2009, **139**, 231–236.
24 T. Guinovart, G. Valdés-Ramírez, J. R. Windmiller, F. J. Andrade and J. Wang, *Electroanalysis*, 2014, **26**, 1345–1353.

25 N. S. Mazlan, M. M. Ramli, M. M. A. B. Abdullah, D. S. C. Halin, S. S. M. Isa, L. F. A. Talip, N. S. Danial and S. A. Z. Murad, *AIP Conf. Proc.*, 2017, 1885.
26 M. H. Banna, H. Najjaran, R. Sadiq, S. A. Imran, M. J. Rodriguez and M. Hoorfar, *Sens. Actuators, B*, 2014, **193**, 434–441.
27 K. Arshak, E. Gillb, A. Arshak and O. Korostynska, *Sens. Actuators, B*, 2007, **127**, 42–53.
28 L. Manjakkal, B. Sakthivel, N. Gopalakrishnan and R. Dahiya, *Sens. Actuators, B*, 2018, **263**, 50–58.
29 J.-C. Chou, S.-J. Yan, Y.-H. Liao, C.-H. Lai, J.-S. Chen, H.-Y. Chen, T.-W. Tseng and T.-Y. Wu, *IEEE Sens. J.*, 2018, **18**, 605–612.
30 A. V. Mamishev, K. Sundara-Rajan, Y. Fumin, D. Yanqing and M. Zahn, *Proc. IEEE*, 2004, **92**, 808–845.
31 K. R. W. Kern, *Handbook of silicon wafer cleaning technology*, 2018.
32 C. Cheng-Hsin, W. Hsun-Pei, C. Cheng-Ho and W. Peng-Rong, *presented in part at the 2011 Fifth International Conference on Sensing Technology*, 2011.
33 S. B. Abel, E. I. Yslas, C. R. Rivarola and C. A. Barbero, *Nanotechnology*, 2018, **29**, 125604.
34 L. Florea, C. Fay, E. Lahiff, T. Phelan, N. E. O'Connor, B. Corcoran, D. Diamond and F. Benito-Lopez, *Lab Chip*, 2013, **13**, 1079–1085.
35 L. Shi, S. Ramsay, R. Ermis and D. Carson, *J. Wound, Ostomy Cont. Nurs.*, 2011, **38**, 514–521.
36 C. A. Cantrell, *Atmos. Chem. Phys.*, 2008, **8**, 5477–5487.
37 W. Du, *Resistive, Capacitive, Inductive, and Magnetic Sensor Technologies*, 2015.
38 R. G. Bates, M. Paabo and R. A. Robinson, *J. Phys. Chem.*, 1963, **67**, 1833–1838.
39 S. Patil, H. Ghadi, N. Ramgir, A. Adhikari and V. R. Rao, *Sens. Actuators, B*, 2019, **286**, 583–590.
40 M. Chung, G. Fortunato and N. Radacsi, *J. R. Soc. Interface*, 2019, **16**, 20190217.

